

# **GSI Annual Report 2005 (extracts)**

## **Chemistry**

### **Gas Chemical Investigation of Hexafluoroacetylacetonates of Zr and Hf with Preseparated Isotopes**

C. E. Düllmann, K. E. Gregorich, I. Dragojevic, R. Eichler, C. M. Folden III, M. A. Garcia, J. M. Gates, D. C. Hoffman, S. L. Nelson, H. Nitsche, G. K. Pang, R. Sudowe

**Page 3**

### **Pb/Hg Separation on the Surface of Au, Pd and Pt**

**Page 4**

A. Yakushev, J. Dvorak, Z. Novackova, A. Türler, B. Wierczinski, W. Brüche, E. Jäger, M. Schädel, E. Schimpf

### **Electrochemical Deposition of Short-lived Pb Isotopes on a Pd Coated Ni Tape**

**Page 5**

H. Hummrich, N. L. Banik, M. Breckheimer, R. Buda, J. V. Kratz, D. Liebe, L. Niewisch, N. Wiehl, W. Brüche, E. Jäger, M. Schädel, B. Schausten, E. Schimpf

### **Simulation of Elution Curves for Chromatography Columns with a Low Number of Theoretical Plates**

**Page 6**

W. Brüche

### **Molecular plating of uranium on thin aluminum backings**

**Page 7**

D. Liebe, K. Eberhardt, J. V. Kratz, P. Thörle, W. Hartmann, A. Hübner, B. Lommel, B. Kindler, J. Steiner

## **Nuclear Structure and Nuclear Decay**

### **Beta decay of $^{101}\text{Sn}$**

**Page 8**

O. Kavatsyuk, C. Mazzocchi, A. Banu, L. Batist, F. Becker, A. Blazhev, W. Brüche, J. Döring, T. Faestermann, M. Gorska, H. Grawe, Z. Janas, A. Jungclaus, M. Karny, M. Kavatsyuk, O. Klepper, R. Kirchner, M. La Commara, K. Miernik, I. Mukha, C. Plettner, A. Plochocki, E. Roeckl, M. Romoli, K. Rykaczewski, M. Schädel, K. Schmidt, R. Schwengner, J. Zylicz

### **Gamow-Teller beta decay of $^{105}\text{Sn}$**

**Page 9**

M. Kavatsyuk, L. Batist, F. Becker, A. Blazhev, W. Brüche, J. Döring, T. Faestermann, M. Gorska, H. Grawe, Z. Janas, A. Jungclaus, M. Karny, O. Kavatsyuk, R. Kirchner, M. La Commara, S. Mandal, C. Mazzocchi, I. Mukha, S. Muralithar, C. Plettner, A. Plochocki, E. Roeckl, M. Romoli, M. Schädel, J. Zylicz

### **Search for the "missing" $\alpha$ -Decay Branch in $^{239}\text{Cm}$**

**Page 10**

Z. Qin, D. Ackermann, W. Brüche, F. P. Hessberger, E. Jäger, P. Kuusiniemi, G. Münzenberg, D. Nayak, E. Schimpf, M. Schädel, B. Schausten, B. Sulignano, X. L. Wu, K. Eberhardt, J. V. Kratz, D. Liebe, P. Thörle, Y. N. Novikov

## **TASCA**

### **The TASCA Project**

**Page 11**

M. Schädel, D. Ackermann, A. Semchenkov, A. Türler

### **Development of the TASCA Control System**

**Page 12**

E. Jäger, W. Brüche, E. Schimpf, M. Schädel, A. Semchenkov, A. Türler, A. Yakushev

### **Modelling the Differential Pumping of the TASCA Gas-Vacuum System**

**Page 13**

A. Semchenkov, W. Brüche, E. Jäger, E. Schimpf, M. Schädel, A. Türler, A. Yakushev

### **TASCA Target Group Status Report**

**Page 14**

K. Eberhardt, J. V. Kratz, D. Liebe, P. Thörle, H.-J. Maier, J. Szerypo, W. Brüche, C. Düllmann, W. Hartmann, A. Hübner, E. Jäger, B. Kindler, B. Lommel, M. Schädel, B. Schausten, E. Schimpf, A. Semchenkov, J. Steiner, A. Türler, A. Yakushev, K. E. Gregorich, R. Sudowe

## **Theory**

### **Fully Relativistic ab initio Calculations of the Electronic Structures of the Superheavy Atoms**

V. Pershina, E. Eliav, U. Kaldor

**Page 15**

**Adsorption of Element 112 on a Au (100) surface**

C. Sarpe-Tudoran, V. Pershina, J. Anton

*Page 16*

**Theoretical Predictions of Complex Formation of Group-4 Elements Zr, Hf, and Rf in H<sub>2</sub>SO<sub>4</sub> Solutions**

V. Pershina, D. Polakova, J. P. Omtvedt

*Page 17*

## Gas Chemical Investigation of Hexafluoroacetylacetonates of Zr and Hf with Preseparated Isotopes

Ch.E. Düllmann<sup>\*,#,\dagger,\ddagger</sup>, K.E. Gregorich<sup>#</sup>, I. Dragojević<sup>#,†</sup>, R. Eichler<sup>§,\parallel</sup>, C.M. Folden III<sup>†,#</sup>, M.A. Garcia<sup>#,†</sup>, J.M. Gates<sup>#,†</sup>, D.C. Hoffman<sup>#,†</sup>, S.L. Nelson<sup>#,†</sup>, H. Nitsche<sup>#,†</sup>, G.K. Pang<sup>#,†,\parallel</sup>, R. Sudowe<sup>#</sup>

<sup>\*</sup>GSI, Darmstadt, Germany; <sup>#</sup>LBL, Berkeley, CA, USA; <sup>†</sup>Univ. California, Berkeley, CA, USA; <sup>§</sup>PSI, Villigen, Switzerland; <sup>\parallel</sup>Univ. Bern, Switzerland; <sup>\ddagger</sup>presently at: MSU, East Lansing, MI, USA.

Gas chemical methods have proven powerful for the investigation of the transactinide elements (TAN,  $Z \geq 104$ ) which are produced in heavy-ion-induced fusion reactions. However, many chemical systems have not been accessible so far due to the plasma caused by the intense heavy-ion beam. Volatile metal complexes containing organic ligands, for example, would be immediately destroyed by this plasma. Recently, preseparation has been used as a new technique to overcome many of the current limitations in TAN chemistry [1,2]. In this technique, nuclear reaction products are separated from the heavy-ion beam and unwanted reaction products in a physical separator, extracted from this separator through a thin window and thermalized in a gas-filled Recoil Transfer Chamber (RTC) [3].

In first experiments conducted at the Lawrence Berkeley National Laboratory (LBL) aiming at the chemical investigation of rutherfordium (Rf,  $Z=104$ ), volatile metal complexes of its lighter homologs hafnium (Hf) and zirconium (Zr) with hexafluoroacetylacetonate (hfa) were studied and some preliminary results are reported here.

Sort-lived ( $T_{1/2}$  between 30 s and 8 min) Zr and Hf isotopes were produced at the LBNL 88-Inch Cyclotron. The nuclear reaction products were preseparated in the Berkeley Gas-filled Separator (BGS) [4] and thermalized in the RTC, which was flushed with hfa-vapor-containing helium and kept at a pressure of  $\sim 1$  bar. The reaction products were transported with the gas flow to an oven installed directly at the exit of the RTC. There, formation of volatile complexes of the type  $M(\text{hfa})_4$  ( $M=\text{Zr}, \text{Hf}$ ) occurred. Single molecules of these complexes are volatile at room temperature and were transported with the gas flow to activated charcoal catchers through a  $\sim 5$ -m long Teflon capillary. The absolute overall yield of this process was measured for  $^{162,165,169}\text{Hf}$ . From these data, the overall "reaction plus transport" time was determined. Two settings were investigated: (i) relatively low hfa concentration and a gas-flow rate of 1.3 l/min, and (ii) relatively high hfa concentration and a gas-flow rate of 2.1 l/min. Preliminary results are shown in Fig. 1 for temperatures up to 400°C. At higher temperatures, decomposition of  $\text{hfa}/M(\text{hfa})_4$  was observed. As can be seen in Fig. 1, the minimum overall time with the current setup under the optimized current conditions is about 40 s.

In isothermal chromatography experiments, the whole 5-m long Teflon capillary was used as chromatography

column. The relative yield of  $^{162}\text{Hf}$  was measured at different isothermal temperatures. The obtained breakthrough curve is shown in Fig. 2. The experiments were modelled using a Monte Carlo Simulation (MCS) [5]. An adsorption enthalpy of  $\text{Hf}(\text{hfa})_4$  on Teflon of  $-\Delta H_{\text{ads}} = (57 \pm 3)$  kJ/mol was evaluated.

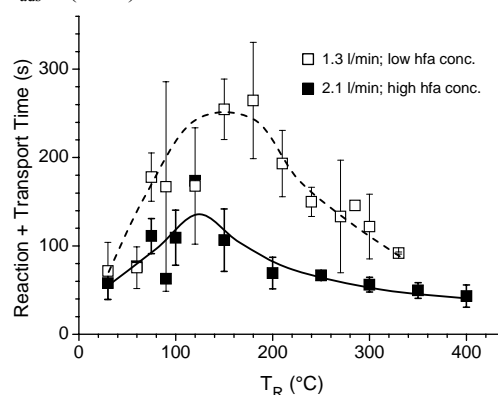


Figure 1: Total time vs. reaction temperature  $T_R$  for  $\text{Hf}(\text{hfa})_4$ . The lines are shown to guide the eye.

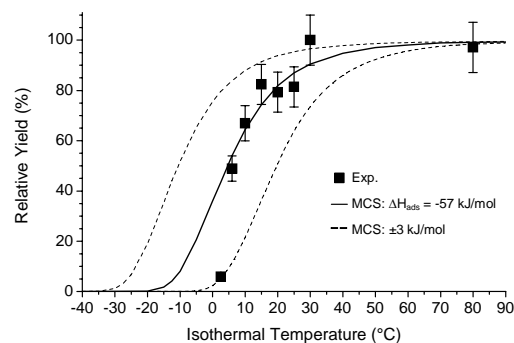


Figure 2: Isothermal chromatogram for  $^{162}\text{Hf}(\text{hfa})_4$ .

### References

- [1] J.P. Omtvedt *et al.*, J. Nucl. Radiochem. Sci. **3** (2002) 121.
- [2] Ch.E. Düllmann *et al.*, Nucl. Instrum. Meth. **A551** (2005) 528.
- [3] U.W. Kirbach *et al.*, Nucl. Instrum. Meth. **A484** (2002) 587.
- [4] V. Ninov *et al.*, AIP Conf. Proc. **455** (1998) 704.
- [5] I. Zvara, Radiochim. Acta **38** (1985) 95.

<sup>\ddagger</sup>C.E.Duellmann@gsi.de

## Pb/Hg Separation on the Surface of Au, Pd and Pt

A. Yakushev, J. Dvorak, Z. Novackova, A. Türler, B. Wierczinski, TUM, München, Germany  
 W. Bröchle, E. Jäger, M. Schädel, E. Schimpf, GSI, Darmstadt, Germany

### Introduction

For experiments with E114 we are developing a method based on the chemical adsorption of E114 on a suitable metal surface followed by the desorption and detection of its  $\alpha$ -decay daughter E112 [1]. To evolve this approach we performed test experiments on the gas chromatography of Pb and Hg to choose suitable materials for chemical filters and to select the best temperature regime. Results from estimates using semi-empirical models for metal-metal interactions between transactinides and transition metals indicate that noble metals are a good choice for the separation of E114 from E112 [2].

### Experimental and results

Short lived isotopes of Pb ( $^{184-189}\text{Pb}$ ) were produced at the UNILAC accelerator using  $^{40}\text{Ar}$  beam and a  $^{152}\text{Gd}$  target. A newly built, heated recoil chamber was employed and the dependence of the Hg yield from the recoil chamber temperature and the carrier gas composition was determined. In Fig. 1 the chemical yield of Hg as a daughter product after alpha-decay of Pb is shown. Hg is a very volatile metal and behaves like an inert gas – i.e. it does not adsorb on inert (oxidized) surfaces, even at room temperature. The upper line shows that some losses of Hg occur due to the adsorption of Pb on the stainless steel (SS) walls of the recoil chamber. At higher temperatures the yield of short-lived Hg isotopes from the recoil chamber increases due to desorption of Pb from the walls and diffusion of implanted daughter atoms back into the gas phase.

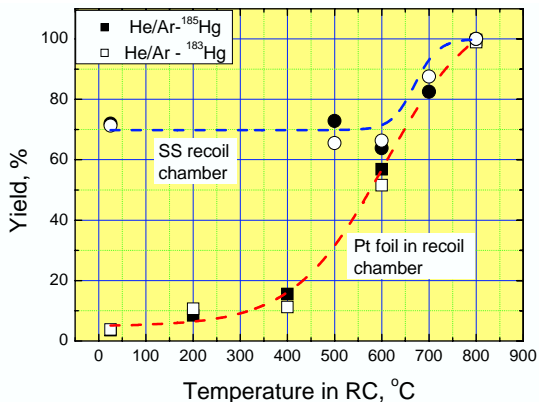


Fig. 1. Yields of  $^{183,185}\text{Hg}$  ( $\alpha$ -decay products of  $^{187,189}\text{Pb}$ ) as a function of the temperature and the exposed surface in the recoil chamber (stainless steel and Pt).

If Pt foil is inserted into the recoil chamber, Hg atoms are chemically adsorbed to the Pt surface at lower temperatures. A desorption of Hg takes place at temperatures well above 500°C.

Next the adsorption/desorption behavior of Pb and Hg nuclides was studied. The recoil chamber (stainless steel surface) was heated to 800°C. The flushed out short-lived Pb and its Hg daughter nuclei were adsorbed on the surface of metallic chromatographic columns, made from Pt, Pd, or Au. Desorption of Pb from the noble metal surface was negligible for temperatures up to 900°C. Desorption of Hg from Pt, Pd and Au surface was studied in the temperature region from room temperature up to 800°C. A typical chromatography curve is shown in Fig. 2. From these curves the enthalpy of adsorption of single Hg atoms on the column surface was evaluated using Monte-Carlo simulations, see Table 1.

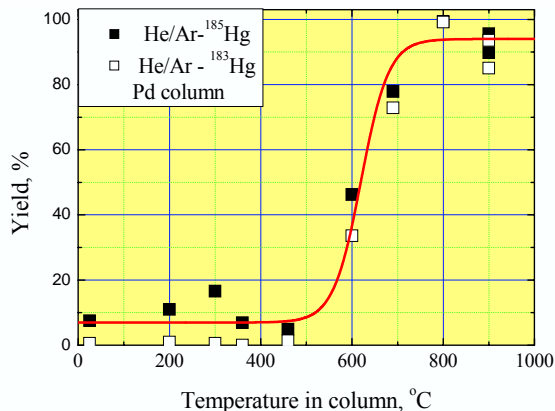


Fig.2. Desorption of Hg isotopes from Pd surface.

Table 1. Adsorption enthalpy of Hg on the surface of Pt, Pd and Au.

Adsorbent	$T_{50\%}, ^\circ\text{C}$	$\Delta H_{\text{ads}}, \text{kJ/mol}$
Platinum	480	$-112 \pm 14$
Palladium	620	$-128 \pm 12$
Gold	630	$-130 \pm 12$

### References

- [1] A. Yakushev et al., GSI Scientific Report 2003, p. 193.
- [2] B. Eichler. Metallochemie der Transaktinoide. PSI-Bericht 00-09, PSI Villigen (2000).

## Electrochemical Deposition of Short-lived Pb Isotopes on a Pd Coated Ni Tape

H. Hummrich, N.L. Banik, M. Breckheimer, R. Buda, J.V. Kratz, D. Liebe, L. Niewisch, N. Wiehl  
 Institut für Kernchemie, Johannes Gutenberg-Universität Mainz, Germany  
 W. Brüchle, E. Jäger, M. Schädel, B. Schausten, E. Schimpf, GSI, Darmstadt

The coupling of the ALOHA system to an electrolytic cell was successfully used to transfer Pb recoil nuclei from a  $^{219}\text{Rn}$  emanation source into the liquid phase with subsequent electrodeposition on Pd electrodes [1].

So far, the transport of the electrodes from the electrolytic cell to the  $\alpha$ -detector was performed manually. However, in an experiment with superheavy elements, an automated transport is necessary, preferably by using a metal tape as the electrode. For the deposition of Pb as the homolog of element 114, the electrode material of choice is Pd [1], but the production of several meters of Pd tape is too expensive. As a cheap and withstanding material, Ni tape is available, but the deposition of Pb on Ni was found to be slow and reversible. To combine the advantages of both materials, Pd was deposited onto a Ni tape (2 cm x 500 cm x 100  $\mu\text{m}$ ), which was wound onto a PE holder to ensure complete contact with the solution. The deposition was carried out in 1.5 L of 0.1 M HCl containing 50 mg/L Pd at -1000 mV vs. Ag/AgCl for 15 min. As counter electrode, a Pt gauze was used.

An electrolytic cell for electrodeposition experiments with tape shaped electrodes was constructed. The metal tape was sealed with two FEP coated o-rings to prevent the liquid from entering the detector system and to ensure a low frictional resistance for a smooth tape transport. A high volume magnetic stir bar was used for agitating the electrolyte. The  $\alpha$ -detector system consisted of three PIN diodes, with (1 x 2) cm active surface, each. The detectors were mounted at 5 cm distance in an Al-case and were kept under He (see Fig.1).

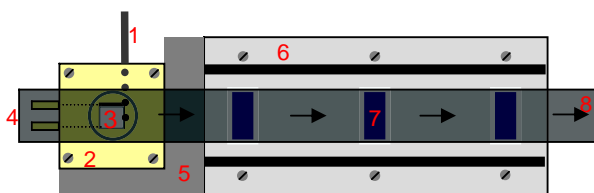


Fig. 1: Schematic of the electrolytic cell with the  $\alpha$ -detection system for electrodeposition and detection of accelerator produced short lived isotopes. 1 Ag/AgCl reference electrode, 2 electrolytic cell with o-rings, 3 high volume magnetic stir bar, 4 electrolyte in- and outlet, 5 spacer, 6 Al-case for detector system, 7 (1 x 2) cm PIN diodes, 8 Pd coated Ni-tape, arrows: stepping direction

The  $\alpha$  emitting  $^{188}\text{Pb}$  ( $t_{1/2} = 25.5$  s) was produced in the reaction  $^{152}\text{Gd} (^{40}\text{Ar}, 4n)$ . A  $^{152}\text{Gd}$  (30% enrichment) target with a thickness of 300  $\mu\text{g}/\text{cm}^2$  on 15  $\mu\text{m}$  Be backing was used. The recoil nuclei were swept out of the recoil chamber by a He/KCl cluster gas-jet at a flow rate of 1.5 L/min and transported through a PE capillary to the ALOHA device. To determine the overall deposition

yield for  $^{188}\text{Pb}$ , the activity was impacted for 3 min on a Kel-F disc. At this collection time, the activity of  $^{188}\text{Pb}$  was nearly in radioactive equilibrium.

After impactation, the disc was switched to the dissolution position and the activity was transferred to the electrolytic cell by continuous cyclic pumping of the electrolyte (0.1 M HCl,  $T = 65^\circ\text{C}$ ).

The rest potential of the Ni(Pd) tape was -250 mV vs. Ag/AgCl. At this potential, Pb deposits spontaneously, so no external potential had to be applied.

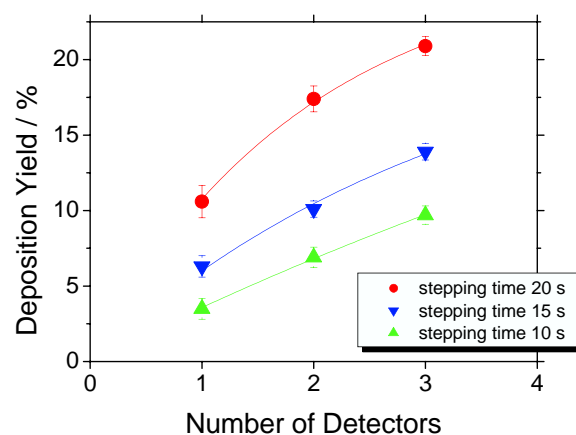


Fig. 2: Deposition yield vs. the number of detectors for various stepping times of the Pd coated Ni tape

The tape was stepped in intervals of 10, 15, and 20 s for several minutes. The deposition yield was calculated by comparing the count rates for each detector with a direct catch on a 0.1  $\mu\text{m}$  nucleopore filter. A maximum deposition yield of 21 % was achieved for a stepping time of 20 s (see Fig. 2).

In this set-up, only three detectors were used. Especially for fast stepping times a big amount of activity was stepped out of the detection system. In a superheavy element experiment, up to 20  $\alpha$  detectors will be available. The yield may be increased significantly by using a pump system with a lower dead volume (now 250  $\mu\text{l}$ ) and a higher electrode surface. The latter can be achieved by using two tapes.

After improving the overall yield, the proposed set-up may be successfully used in aqueous chemistry with element 114. Experiments with homologs suggest, that also the electrochemical deposition of element 108 - 111, 113, 115, and 116 should be possible.

## References

- [1] Hummrich et al., *GSI Scientific Report 2004*, p. 189

## Simulation of Elution Curves for Chromatography Columns with a Low Number of Theoretical Plates

W. Brüchle, GSI, Darmstadt, Germany

Chromatographic techniques are among the most effective chemical methods to separate and characterize closely related chemical substances or ions. More than half a century ago the main theoretical fundamentals for these methods were developed; even a Nobel Prize was awarded to Martin and Synge [1] for their theoretical and practical methodic developments. There is a lot of pioneering theoretical descriptions of peak position and peak width, often based on the molecular dynamic theory of chromatography, originally developed by Giddings and Eyring [2]. The model represents the progress of a single molecule through the column as a chain of elementary adsorption-desorption stochastic processes. The majority of these papers have started with partial differential equations leading to Bessel functions. The asymptotic expansion of the Bessel functions weighed by the probability of the initial state of the molecule should yield the distribution curve for the elution. Rather complicated calculations using the characteristic function method are described in [3]. An easier way to describe the chromatographic process is the "theoretical plate" concept. It is the imaginary section of a column in which a complete equilibrium step takes place. The model was successfully used in [1] for liquid-solid chromatography. In most cases textbooks dealing with chromatography will present the following formula without derivation:

$$K_d = (T_r - T_0) * F / m = (V - V_0) / m \quad (1)$$

with  $T_r$  = retention time  
 $T_0$  = column hold-up time due to the free column volume  
 $F$  = flow rate of the mobile phase [mL/min]  
 $m$  = mass of the stationary phase (ion exchanger, reversed phase material) [g]  
 $K_d$  = partition coefficient (distribution coefficient)  
 $V_p$  = volume eluted until the peak maximum [mL]  
 $V_0$  = free column volume (dead volume) [mL]

During series of fast automated separations on rather small chromatographic columns (1.6 mm i.d., 8 mm long, and 1mm i.d., 3.5 mm long) with the ARCA and the AIDA systems [4,5] it was noticed that the peak shapes differed from a Gaussian; in addition it was often not possible to measure complete elution curves, but only two fractions. Still the distribution coefficient  $K_d$  should be determined. In [5] the Glueckauf equation of chromatography was used [6]:

$$A(V) = A_{max} \exp(-N (V_p - V)^2 / 2V_p V) \quad (2)$$

where  $N$  is the number of theoretical plates. In a new stepwise simulation some discrepancies occurring in some pioneering publications could be removed. Some authors stated, that a dead volume of a chromatographic column is only the result of the discontinuous

treatment, and with a  $K_d=0$  the elution would start immediately without delay [6]. This problem could be solved by starting the simulation with the last theoretical plate, and going upwards with the calculation. The activity transported from plate number  $i$  to the next plate  $i+1$  is given by:

$$\Delta a = a(i)(1 - K_d / (K_d + r_v)) \quad (3)$$

In this formula,  $r_v$  is the ratio of the free column volume to the mass of the exchanger material  $v_l/m$ . The results of the simulation shows an obvious similarity of the elution curves with the Poisson-curves from [7]. A numerical comparison shows that the elution curves can very well be described by:

$$A(V - V_0) = A_{max} * \mu^{(N-1)} / (N-1)! * \exp(-\mu) \quad (4)$$

$$\text{with } \mu = (V - V_0) * N / (m * K_d)$$

One can determine the  $K_d$ -value from the peak of the Poisson curve using:

$$K_d = (V - V_0) * N / (N - 1) / m \quad (5)$$

The difference to the classical formula is the factor  $N/(N-1)$ , that can be neglected for longer columns. The Glueckauf equation gives reasonable fits when a shift by  $V_0$  is added.

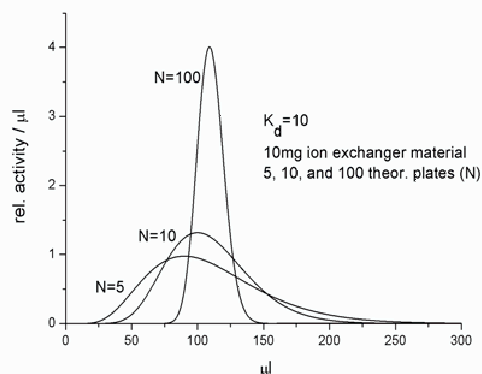


Figure 1: Simulation for different number of plates

### References

- [1] A.J.P. Martin, R.L.M. Synge, *Biochem J.* **35**, 1358-1368 (1941)
- [2] J.C. Giddings, H. Eyring, *J. Phys. Chem.* **59**, 416-421 (1955)
- [3] A. Cavazzini, M. Remelli, F. Dondi, *J. Micro Sep.* **9**, 295-302 (1997)
- [4] M. Schädel, *Radiochim. Acta* **89**, 721-728 (2001) and references therein
- [5] H. Haba *et al.*, *J. Am. Chem. Soc.* **126** (16) 5219-5224 (2004)
- [6] E. Glueckauf, *Trans. Faraday* **51**, 34-44 (1955)
- [7] W. Brüchle, *Radiochim. Acta* **91**, 71-80 (2003)

## Molecular plating of uranium on thin aluminum backings\*

D. Liebe, K. Eberhardt, J.V. Kratz, P. Thörle, Institut für Kernchemie,  
Johannes-Gutenberg-Universität Mainz (UMZ), Germany

W. Hartmann, A. Hübner, B. Lommel, B. Kindler, J. Steiner, GSI, Darmstadt, Germany

Molecular plating is widely used for the deposition of lanthanide and actinide compounds on thin metallic backing foils [1]. At GSI and UMZ, this method has been previously applied on Ti or Be foils. Within the requirements of the TASCA-Project (TransActinide Separator and Chemistry Apparatus) very thin foils of Al (2-10 $\mu$ m) as backing material have been proposed [2].

The general usability of very thin Al was investigated by a test series with Gd and U. For these tests, plating conditions were adopted unchanged from previous practices [3]. Although Al foils of less than 10 $\mu$ m in thickness are difficult to manage, they show no significant disadvantages compared to Ti or Be with molecular plating.

2-Propanol (isopropanol) as organic solvent has previously been used for the preparation of actinide targets on Ti and Be backings. But on Al, the stability of the U layer is not acceptable. The surface of most of the targets looked scaly or cracked associated with irreproducible plating yields. In order to solve these problems, an alternative solvent, 2-Methyl-1-Propanol (isobutanol) was tested. Table 1 compares the plating condition of the previously used isopropanol and the newly tested conditions applying isobutanol.

Table 1: Plating conditions for isopropanol and isobutanol (U on Al-Backing)

Solvent	Voltage [V]	Current [mA]	Plating time [h]	Thickn. [ $\mu$ g/cm <sup>2</sup> ]
Iso-propanol	100-1200 stepwise	0.5 -3.0	1	390 <sup>#</sup>
Iso-butanol	150 V	0.01-0.5	4 - 5	650 <sup>##</sup>

The hygroscopic character of isopropanol might have been the reason for the poor surface quality since the plating solution as always been exposed to air for a couple of hours prior to the plating. The content of water may cause the relative high current and, thus, it possibly effects the formation of obstructing hydroxides at the surface of the backing foil. Isobutanol, which is also used by the target laboratory of the Lawrence Berkeley National Laboratory, LBNL, is less polar and therefore poorly water-soluble [4]. During numerous experiments, the plating conditions were adjusted to a lower voltage resulting in a longer plating time as shown in Table 1.

\* F+E Vertrag Mz/JVK Entwicklung und Herstellung von Transuran- u. sonstigen radioaktiven Targets

# corresponds to 74% at an intake of 500 $\mu$ g U /cm<sup>2</sup>

## corresponds to 65% at an intake of 1000 $\mu$ g U/cm<sup>2</sup>

With isobutanol, the coating looks more homogenous without visible cracks. That has been approved with 25 $\mu$ m as well as 10 $\mu$ m Al backings. Fig 1 shows a light optical micrograph of an U-target, as usually prepared for the existing rotating actinide target wheel assembly at GSI.

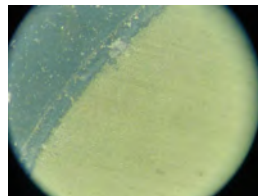


Fig 1: Uranium on Al Backing (25 $\mu$ m), plated from isobutanol within 3 h, Voltage 150 V

Furthermore, for U, a time dependence of the depositions yield has been determined. So far, a maximum yield at about 60 - 65 % is reached at a plating time of 5 h, as shown in Fig 2. In future investigations, the work will also focus on an increase of deposition yield to 75 % or more as achieved with isopropanol.

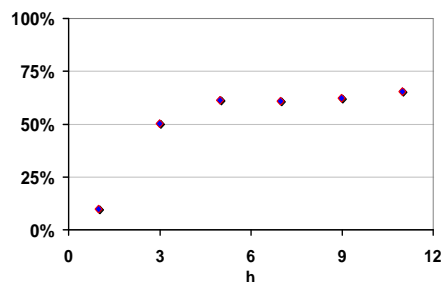


Fig 2: Time dependence of deposition yield at molecular plating of U on 25 $\mu$ m Al backing (from isobutanol with 150 V)

Next we plan to apply these conditions to other elements, especially various lanthanides. Also, the use of autoradiography [5] and REM/EDX will be further investigated to monitor target thickness, homogeneity and surface layer composition, respectively.

### References

- [1] W. Parker, R.Falk, Nucl. Instr and Meth 16 (1962), 355
- [2] M. Schädel et al., contribution to this report
- [3] D.Liebe, P. Thörle, J.V. Kratz "Further investigations on target preparation for heavy element studies", Annual report 2004, Institut f. Kernchemie, Universität Mainz, 2005
- [4] P.M. Zielinsky, K. E. Gregorich, R. Sudowe, private communication at LBNL, Berkeley, March 2005
- [5] K. Eberhardt et al., contribution to this report

## Beta decay of $^{101}\text{Sn}$

O. Kavatsyuk<sup>a,b</sup>, C. Mazzocchi<sup>a,c</sup>, A. Banu<sup>a</sup>, L. Batist<sup>d</sup>, F. Becker<sup>a</sup>, A. Blazhev<sup>a</sup>, W. Bröchle<sup>a</sup>, J. Döring<sup>a</sup>, T. Faestermann<sup>e</sup>, M. Górska<sup>a</sup>, H. Grawe<sup>a</sup>, Z. Janas<sup>f</sup>, A. Jungclaus<sup>g</sup>, M. Karny<sup>f</sup>, M. Kavatsyuk<sup>a,b</sup>, O. Klepper<sup>a</sup>, R. Kirchner<sup>a</sup>, M. La Commara<sup>h</sup>, K. Miernik<sup>f</sup>, I. Mukha<sup>a</sup>, C. Plettner<sup>a</sup>, A. Płochocki<sup>f</sup>, E. Roeckl<sup>a</sup>, M. Romoli<sup>h</sup>, K. Rykaczewski<sup>i</sup>, M. Schädel<sup>a</sup>, K. Schmidt<sup>a</sup>, R. Schwengner<sup>k</sup>, J. Żylicz<sup>f</sup>

<sup>a</sup>GSI, Darmstadt, Germany; <sup>b</sup>National Taras Shevchenko Univ. of Kyiv, Ukraine; <sup>c</sup>Univ. of Tennessee, Knoxville, USA; <sup>d</sup>PNPI, Gatchina, Russia; <sup>e</sup>TU, München, Germany; <sup>f</sup>Univ. of Warsaw, Poland; <sup>g</sup>Instituto Estructura de la Materia, CSIC and Departamento de Física Teórica, UAM Madrid, Spain; <sup>h</sup>Università "Federico II" and INFN, Napoli, Italy; <sup>i</sup>ORNL, Oak Ridge, USA; <sup>k</sup>IKHP, FZ Rossendorf, Dresden, Germany

The  $\beta$  decay of the very neutron-deficient isotope  $^{101}\text{Sn}$ , one of the four closest neighbours of the doubly-magic nucleus  $^{100}\text{Sn}$ , was studied at the GSI on-line mass separator.  $^{101}\text{Sn}$  was produced in the fusion-evaporation reaction induced by a 36 particle-nA,  $\sim 5$  MeV/u  $^{58}\text{Ni}$  beam on a  $^{50}\text{Cr}$  target. By adding  $\text{CS}_2$  vapour to the ion source, high chemical selectivity for tin was achieved [1], thus strongly suppressing the isobaric contaminants. After ionisation and acceleration to 55 keV, the  $A=101+32$  ions were mass separated and implanted either into thin carbon foils in front of a setup for measuring  $\beta$ -delayed protons ( $\beta\text{p}$ ) or into a tape positioned in the centre of an array of silicon and germanium detectors (Si-Ge array) for  $\beta$ -delayed  $\gamma$ -ray ( $\beta\gamma$ ) spectroscopy.

In the  $\beta\text{p}$  experiment the  $A=101+32$  beam was periodically switched between two carbon foils in consecutive grow-in (12 s) and decay (12 s) intervals, the collected  $\beta\text{p}$  activity being recorded by two  $\Delta E$ - $E$  Si-detector telescopes ( $\Delta E$ : 450 mm<sup>2</sup>, 20  $\mu\text{m}$ ;  $E$ : 2000 mm<sup>2</sup>, 500  $\mu\text{m}$ ). Each of them covered a solid angle of 17(2) %. The  $\beta\text{p}$  data allowed us to redetermine with improved accuracy the half-life of  $^{101}\text{Sn}$  to be  $1.9 \pm 0.3$  s and to estimate the production cross-section in the  $^{50}\text{Cr}(^{58}\text{Ni}, \alpha 3\text{n})$  fusion-evaporation reaction to be about 60 nb.

In the  $\beta\gamma$  experiment, three Si detectors (two 30 mm $\times$ 30 mm and one 14 mm $\times$ 14 mm) were placed inside of a small vacuum chamber, covering the solid angle of about 40 %. Around this chamber two GSI VEGA-SuperClover detectors and one small Clover detector (i.e. a total of 12 Ge crystals) were mounted, yielding a total photopeak efficiency of 7.5 % at 1.3 MeV. The measurement was performed while the  $A=101+32$  beam was continuously implanted into the tape at rest. Every 8 s the activity was removed from the implantation position. The  $\beta\gamma$  data yielded for the first time weak evidence for the observation of  $\beta$ -delayed  $\gamma$  rays of  $^{101}\text{Sn}$  which apparently form a cascade of 352 and 1065 keV transitions in  $^{101}\text{In}$ .

Figure 1 shows the experimental  $\beta\text{p}$  energy spectrum together with theoretical predictions. The calculated spectra were obtained on the basis of estimated  $Q_{EC}$  and  $S_p$  val-

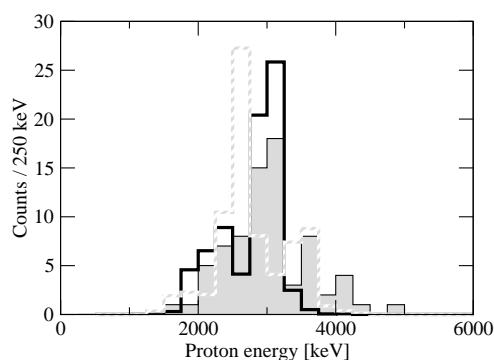


Figure 1: Experimental energy spectrum of  $\beta$ -delayed protons compared to predictions obtained on the basis of a shell-model calculation assuming a  $5/2^+$  (solid-line histogram) and  $7/2^+$  (dashed-line histogram) spin-parity assignment for the  $^{101}\text{Sn}$  ground-state. Theoretical and experimental spectra are normalised to equal integral number of counts.

ues [2], a  $\beta$ -intensity distribution as predicted by a shell-model calculation [3] and a barrier-transmission calculation based on a statistical model [4]. The centre of gravity of the experimental  $\beta\text{p}$  energy spectrum is in good agreement with the prediction based on the  $5/2^+$  assignment for the ground-state of  $^{101}\text{Sn}$ . In contrast, the theoretical spectrum obtained for a  $7/2^+$  assignment is concentrated in a more narrow energy range, the main intensity lying about 400 keV lower. Although, the theory based assignment of the ground-state of  $^{101}\text{Sn}$  and the lowest-lying orbital above the  $N = 50$  shell-closure is unambiguously a  $5/2^+$ , the shell-model calculation [3] overestimate the energy of the GT resonance in  $^{103}\text{Sn}$  by 500 keV.

[1] R. Kirchner, NIM B **204**, 179 (2003).

[2] G. Audi *et al.*, Nucl. Phys. A **729**, 337 (2003).

[3] M. Hjorth-Jensen *et al.*, Phys. Rep. **251**, 125 (1995).

[4] B. Jonson *et al.*, Proc. 3rd Intern. Conf. on Nuclei far from Stability, Cargèse (1976), CERN 76-13, p.277; P. Hornshøj *et al.*, Nucl. Phys. A **187**, 609 (1972).

## Gamow-Teller beta decay of $^{105}\text{Sn}$

M. Kavatsyuk<sup>a,b</sup>, L. Batist<sup>c,d</sup>, F. Becker<sup>a</sup>, A. Blazhev<sup>a,e</sup>, W. Brüche<sup>a</sup>, J. Döring<sup>a</sup>, T. Faestermann<sup>f</sup>,  
 M. Górska<sup>a</sup>, H. Grawe<sup>a</sup>, Z. Janas<sup>g</sup>, A. Jungclaus<sup>h</sup>, M. Karny<sup>g</sup>, O. Kavatsyuk<sup>a,b</sup>, R. Kirchner<sup>a</sup>,  
 M. La Commara<sup>d</sup>, S. Mandal<sup>a</sup>, C. Mazzocchi<sup>a</sup>, I. Mukha<sup>a,i</sup>, S. Muralithar<sup>a,k</sup>, C. Plettner<sup>a</sup>,

A. Płochocki<sup>g</sup>, E. Roeckl<sup>a</sup>, M. Romoli<sup>d</sup>, M. Schädel<sup>a</sup>, J. Żylicz<sup>g</sup>

<sup>a</sup>GSI, Darmstadt, Germany; <sup>b</sup>National Taras Shevchenko Univ. of Kyiv, Ukraine;

<sup>c</sup>PNPI, St. Petersburg, Russia; <sup>d</sup>Università "Federico II" and INFN, Napoli, Italy;

<sup>e</sup>University of Sofia, Bulgaria; <sup>f</sup>TU, München, Germany; <sup>g</sup>Univ. of Warsaw, Poland;

<sup>h</sup>Departamento de Física Teórica, UAM Madrid, Spain; <sup>i</sup>Kurchatov Institute, Moscow, Russia;

<sup>k</sup>Nuclear Science Center, New Delhi, India

The interest in studying nuclei in the  $^{100}\text{Sn}$  region, in particular those "south-east" of this doubly magic shell closure, is partly motivated by the occurrence of a resonance-like  $\beta$  decay related to the Gamow-Teller (GT) transitions of a  $g_{9/2}$  proton into a  $g_{7/2}$  neutron. For odd-A tin isotopes, this transformation initiates from the even-even core, leading to three-quasiparticle states in the odd-Z, even-N daughter nucleus and a correspondingly complex structure of the GT resonance. A suitable tool for measuring the  $\beta$ -intensity distribution in such cases is total absorption spectroscopy. This method is based on recording cascades of  $\beta$ -delayed  $\gamma$  rays rather than single  $\gamma$  transitions. This allows one to determine the entire  $\beta$ -intensity distribution, including weak  $\beta$  transitions to high-lying excited states in the daughter nucleus. In this work a total absorption spectrometer (TAS) [1] was used for investigating the  $^{105}\text{Sn}$  decay. The motivation for this study was to improve the data available from previous experiments on the  $\beta$ -delayed  $\gamma$  [2] and proton ( $\beta p$ ) [3] emissions of  $^{105}\text{Sn}$ , with the aim of determining the GT strength distribution and comparing it with shell-model predictions.

The experimental technique and data analysis procedure were the same as used for  $^{103}\text{Sn}$   $\beta$ -decay study, described in ref. [4]. With this investigation a dominant GT resonance occurring in the decay of  $^{105}\text{Sn}$  was identified, peaking at 3.6 MeV and having a width of 300 keV. In fig. 1 the experimental GT strength distribution is compared with shell-model calculation based on an empirical interaction [5], yielding qualitative agreement with the shape of the measured GT resonance. However, the theoretical distribution is shifted by about 600 keV towards lower excitation energies, and the predicted summed GT strength is 4.5(6) times higher than the experimental one of 3.0(4) in units of  $g_A^2/4\pi$ . This hindrance is in agreement with the values obtained for other nuclei in the  $^{100}\text{Sn}$  region. The shift may be ascribed to the inverted  $d_{5/2} - g_{7/2}$  sequence in  $^{101}\text{Sn}$  and/or a reduced neutron pairing in the shell model approach.

In addition the TAS allowed us to measure further decay characteristics of  $^{105}\text{Sn}$  such as the  $Q_{EC}$  value of 6230(80) keV [6] and the contribution of 0.420(35) of the electron capture process to the total decay rate. The  $^{105}\text{Sn}$  half-life of 32.7(5) s was remeasured with higher precision.

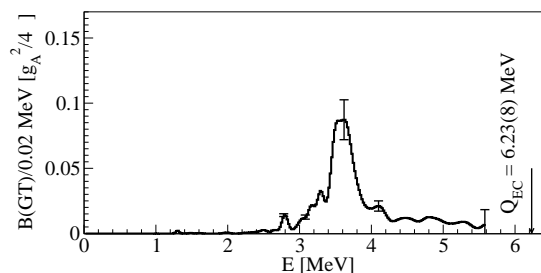


Figure 1: Gamow-Teller strength distribution for  $^{105}\text{Sn}$  obtained from the TAS measurement (black-line histogram) and from the shell-model calculation (dotted histogram). The theoretical distribution was normalised to the experimental summed GT strength (see text).

The  $\beta p$  emission was detected using the ancillary silicon detectors of the TAS. This allowed us to measure the  $\beta p$  branching ratio to be  $1.1(4) \times 10^{-4}$ .

Using the main TAS crystal as an active background shielding for the ancillary germanium and silicon detectors, conversion coefficients of 0.055(6) and 0.07(2) were determined for the long-lived  $1/2^-$  isomers in  $^{105}\text{In}$  and  $^{103}\text{In}$  that have excitation energies of 632 and 674 keV, respectively. A comparison of this result with the theoretical values of 0.062 and 0.075 [7], respectively, suggests  $M4$  polarity of the transition. This confirms the previous multipolarity assignment [8].

## References

- [1] M. Karny *et al.*, Nucl. Instr. Meth. B **126**, (1997) 411.
- [2] M. Pfützner *et al.*, Nucl. Phys. A **581**, (1995) 205.
- [3] P. Tidemand-Petersson *et al.*, Z. Phys. A **302**, (1981) 343.
- [4] O. Kavatsyuk *et al.*, Eur. Phys. J. A **25**, (2005) 211.
- [5] K. Rykaczewski, GSI-95-09 (1995), B.A. Brown, K. Rykaczewski, Phys. Rev. C **50**, (1994) R2270.
- [6] M. Kavatsyuk *et al.*, Intern. J. Mass Spectrometry, in print.
- [7] I.M. Band *et al.*, Atomic Data and Nuclear Data Tables **81**, (2002) 1.
- [8] J. Verplancke *et al.*, Z. Phys. A **315**, (1984) 307.

## Search for the "missing" $\alpha$ -Decay Branch in $^{239}\text{Cm}$

Z. Qin<sup>1,3</sup>, D. Ackermann<sup>1</sup>, W. Bröchle<sup>1</sup>, F.P. Hessberger<sup>1</sup>, E. Jäger<sup>1</sup>, P. Kuusiniemi<sup>1</sup>, G. Münzenberg<sup>1</sup>, D. Nayak<sup>1</sup>, E. Schimpf<sup>1</sup>, M. Schädel<sup>1</sup>, B. Schausten<sup>1</sup>, B. Sulignano<sup>1,2</sup>, X.L. Wu<sup>1,3</sup>, K. Eberhardt<sup>2</sup>, J.V. Kratz<sup>2</sup>, D. Liebe<sup>2</sup>, P. Thörle<sup>2</sup>, Yu. N. Novikov<sup>1,4</sup>

<sup>1</sup>GSI, Darmstadt, Germany, <sup>2</sup>Johannes Gutenberg-Universität, Mainz, Germany, <sup>3</sup>IMP, Lanzhou, P.R. China, <sup>4</sup>Petersburg Nuclear Physics Institute, Gatchina, Russia

We continued our search for the "missing"  $\alpha$ -decay branch of  $^{239}\text{Cm}$  in a series of irradiations at the UNILAC making use of the  $^{232}\text{Th} (^{12}\text{C}, 5n)^{239}\text{Cm}$  reaction and applying nuclear chemistry techniques. The goal of these experiments and a description of the irradiation and detection techniques were reported in Ref. [1]. In our recent experiments,  $^{12}\text{C}$  beam intensities varied between 0.4 and 0.6 particle  $\mu\text{A}$  (available as a parasitic beam during nighttimes). Each irradiation lasted between 4 and 6 h. The radiochemical separation procedure [2] to prepare a purified Cm sample for  $\alpha$ -spectroscopy was accomplished within 2.5 h.

The yield of extraction and precipitation was checked by adding  $^{170}\text{Tm}$  radiotracer and was found to be typically about 75%. The yield of the evaporation step was determined with  $^{151}\text{Pm}$  (product of  $^{12}\text{C}$  induced  $^{232}\text{Th}$  fission) and, for the evaluated experiments, it was close to 100%. The total chemical yield was assumed to be about 70% for curium. Samples were assayed for  $\alpha$ -activities by 450  $\text{mm}^2$  PIPS detectors. The energy resolution of the evaporated samples was 60 keV (FWHM). All  $\alpha$ -events were recorded together with detector numbers and associated times and were stored in a list mode.

In our recent series of experiments, two different  $^{12}\text{C}$  beam energies were applied. 74 MeV (middle of target) was chosen as the first energy to reproduce our previous results and to increase the statistics. This energy is close to the maximum of the  $^{239}\text{Cm}$  ( $5n$ ) excitation function and it allows monitoring the stability of the experiment through the observation of  $^{240}\text{Cm}$  and  $^{238}\text{Cm}$  in  $4n$  and  $6n$  channel. Fig. 1(a) shows a typical  $\alpha$ -spectrum of a Cm fraction obtained at 74 MeV and recorded for the first 10 hours.  $^{240}\text{Cm}$  with  $\alpha$ -energies of 6.29 and 6.25 MeV is clearly observed. A second, weaker  $\alpha$ -peak around 6.52 MeV can be assigned to  $^{238}\text{Cm}$ . A few events were observed in the region between 6.30 and 6.50 MeV, interesting for  $^{239}\text{Cm}$ . However, tailing of  $^{238}\text{Cm}$  into this region cannot be excluded. The time distribution of these events provides no additional information as  $^{238}\text{Cm}$  and  $^{239}\text{Cm}$  have very similar half-lives.

To be more sensitive in the interesting energy range, we lowered the beam energy to 70 MeV. In agreement with HIVAP calculations, which predict the  $6n$  cross section to decrease by three orders of magnitude from 74 to 70 MeV - the  $5n$  cross section should only be lowered by a factor of two or less -, no  $^{238}\text{Cm}$  was observed anymore; see Fig. 1(b). Due to a smaller beam integral, the  $^{240}\text{Cm}$  peak,

which dominates the spectrum with energies of 6.29 and 6.25 MeV, is less intense in Fig. 1(b) as in Fig. 1(a).

No  $\alpha$  events with energies between 6.30 and 6.50 MeV, which could be assigned to  $^{239}\text{Cm}$ , were observed in this experiment at 70 MeV. From this we conclude that the corresponding  $\alpha$ -events observed at 74 MeV  $^{12}\text{C}$  energy were tails of the  $^{238}\text{Cm}$  peak caused by self-absorption effects of the  $\alpha$  source prepared by evaporation.

Cross sections were calculated from measured  $\alpha$  activities, the  $^{232}\text{Th}$  target thickness, beam integrals, and assuming that 100% of the Cm recoiled out of the target and was caught in the Cu catcher foil. As the measured cross section ratio of  $\sigma_{4n}:\sigma_{6n}$  at 74 MeV is consistent with HIVAP results ( $\sigma_{4n}:\sigma_{6n}=1:16$ ) within a factor of 2 we trust the HIVAP  $\sigma_{4n}:\sigma_{5n}=1:1$  ratio. From this, the total number of  $^{240}\text{Cm}$   $\alpha$ -events and the non-observation of  $^{239}\text{Cm}$  (taking 3 events for a 95% confidence limit) we calculated an upper limit of  $3 \times 10^{-5}$  for a  $^{239}\text{Cm}$   $\alpha$ -branch.

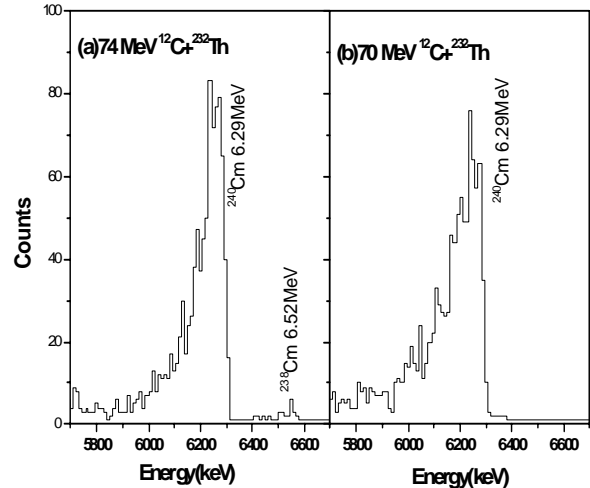


Figure 1:  $\alpha$ -spectra of Cm fractions, for the first 10 h measuring time, from the reaction of (a) 74 MeV and (b) 70 MeV  $^{12}\text{C} + ^{232}\text{Th}$ .

## References

- [1] Z. Qin et al, GSI Scientific Report 2004, p. 75
- [2] Z. Qin et al., GSI Scientific Report 2004, p. 190, 191

## The TASCA Project

M. Schädel<sup>1</sup>, D. Ackermann<sup>1</sup>, A. Semchenkov<sup>1,2</sup>, and A. Türler<sup>2</sup> for the TASCA collaboration  
<sup>1</sup>GSI Darmstadt, Germany; <sup>2</sup>TUM Garching, Germany

The TransActinide Separator and Chemical Apparatus, **TASCA**, project started early in 2005. The envisioned research program will focus on the separation and investigation of neutron-rich transactinide nuclides produced in hot-fusion reactions with actinide targets. While novel chemical investigations of transactinide elements - after pre-separation with a physical recoil separator - is one of the main goals, a rich nuclear structure investigation program is foreseen complemented by typical hot-fusion nuclear reaction studies; see [1] for a coverage of preparatory and ongoing activities.

As the central device for all these research programs we opted for a gas-filled separator [2] making at least partially use of existing components from the former NASE [3]. To optimize all separator components, new and old ones, ion-optical calculations were performed [2] based on the model fusion reaction of 5-6 MeV/u <sup>48</sup>Ca on 0.5 mg/cm<sup>2</sup> actinide targets (<sup>238</sup>U, <sup>244</sup>Pu).

The DQ<sub>h</sub>Q<sub>v</sub> configuration, which was selected as the best choice [2], allows operation in two possible modes. While the DQ<sub>h</sub>Q<sub>v</sub> mode gives the highest possible transmission the smallest image size results from the DQ<sub>v</sub>Q<sub>h</sub> mode. New ducts were designed and built for the dipole and the quadrupoles to maximize the transmission in both modes.

For the "high transmission" DQ<sub>h</sub>Q<sub>v</sub> mode, see Fig. 1, a horizontal and vertical acceptance of 110 and 40 mrad is achieved which corresponds to a solid angle of 13.3 msr. Assuming a 30% reduction for the operation as a gas-filled separator, a transmission of about 45% is estimated which would yield a slightly higher value as compared with the Dubna gas-filled separator, DGRRS, or GARIS at RIKEN. With a dispersion of 9 mm/% a "vacuum" image area of 27 cm<sup>2</sup> is calculated.

In the DQ<sub>v</sub>Q<sub>h</sub> mode a reduced horizontal acceptance of 34 mrad presumably yields only 30% transmission. However, an extraordinarily small image area of 7 cm<sup>2</sup> (in vacuum) should be achievable - a key issue to build small recoil transfer chambers for a fast transport of products into any chemistry set-ups and something unique for TASCA. Monte-Carlo simulations [4] making use of existing models of the dipole and quadrupole magnets [5] are under way.

All magnets, including ducts and water cooling, are now installed in the newly built cave at the UNILAC beam line X8, and they are connected to power supplies. A LabVIEW control program and communication via MIL-bus was established and first tests of the power supplies and magnets are promising. The control program for the power supplies will be part of a general TASCA control program described in a separate contribution [6].

To make use of highest available beam intensities, a windowless differential pumping section was installed and successfully tested. Details are given elsewhere [7].

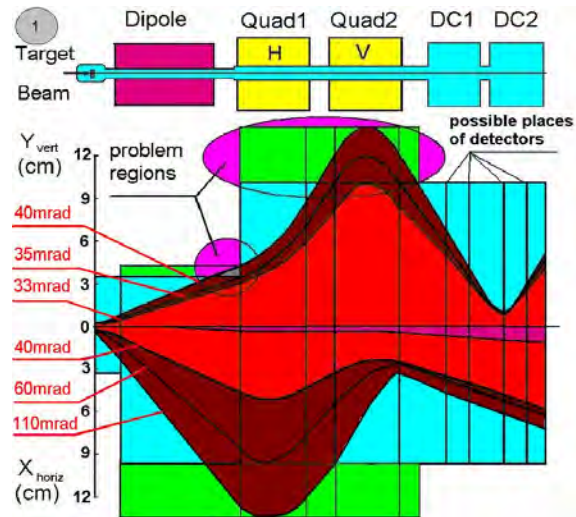


Figure 1: DQ<sub>h</sub>Q<sub>v</sub> configuration and simulation for the vertical and horizontal beam shape. Inner lines demonstrate constraints from the old NASE set-up. Outer lines show the present TASCA situation with new ducts.

A new target chamber was designed and built which accommodates (i) the rotating actinide target wheel in an easily removable cassette, (ii) the newly built drive [8], (iii) collimators, and (iv) beam diagnostic components. A beam current transformer upstream of the target shall allow for continuous monitoring of the beam current.

Last not least it is important to mention not only the new TASCA cave at X8 with its concrete shielding - designed and built for the highest envisioned beam intensities - and its access system, but also all the infrastructure components - a crane, electrical power for magnets, pumps, detectors and data acquisition systems, cooling water, pressurized air and nitrogen, filtered exhaust systems, air conditioning, and many other components - which were installed in 2005 [9].

## References

- [1] <http://www.gsi.de/tasca>; <http://www.gsi.de/tasca05>
- [2] A. Semchenkov et al., GSI Scientific Report 2004, GSI Report 2005-1, p. 332.
- [3] V. Ninov et al., Nucl. Instr. Meth. A 357 (1995) 486.
- [4] K. E. Gregorich, private communication.
- [5] T. Belyakova et al., GSI Scientific Report 2004, GSI Report 2005-1, p. 333.
- [6] E. Jäger et al., contribution to this report.
- [7] A. Semchenkov et al., contribution to this report.
- [8] H.-J. Schött, E. Jäger, private communication.
- [9] Many thanks to everybody who contributed to this.

## Development of the TASCA Control System

E. Jäger<sup>1</sup>, W. Brühle<sup>1</sup>, E. Schimpf<sup>1</sup>, M. Schädel<sup>1</sup>, A. Semchenkov<sup>1,2</sup>, A. Türler<sup>2</sup>, A. Yakushev<sup>2</sup>  
<sup>1</sup>GSI, Darmstadt, Germany, <sup>2</sup>TUM Garching, Germany

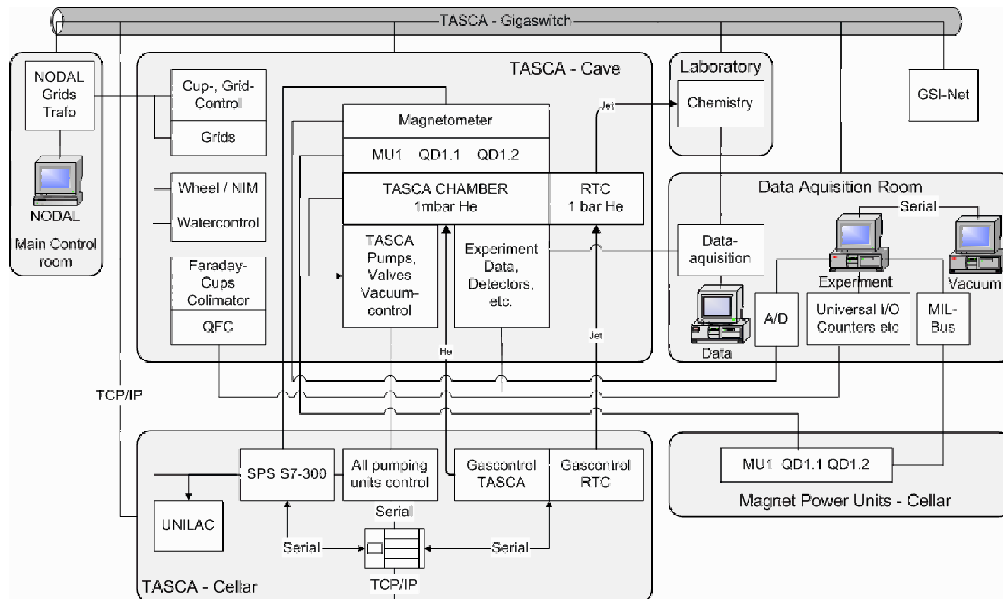


Fig.1. Scheme of the TASCA control system presently under development.

The TASCA [1] control system will be based on Siemens SPS microcontrollers as low level control units, and PCs for the high level control. For safety reasons we opted for SPS controllers at the lower level. All safety critical fast signals like interlocks will be processed by hardware components or by the SPS. PCs will be applied as the user interface and to control processes which are not time critical, like the routine operation of the pumping system, magnet controls, beam current reading and others. High level programming will be performed under LabVIEW.

The common scheme of the TASCA control system is presented in Fig.1. It consists of modules to control (i) dipole and quadrupole magnets, (ii) gas pressures and differential pumping, and (iii) all heavy-ion beam and irradiation related aspects including the target wheel control. Communication links will be established to the NODAL system, our data acquisition system and automated chemistry set-ups.

Components of the control system will be located in (i) the TASCA cave, (ii) the cellar below TASCA, (iii) the data acquisition room, (iv) the UNILAC control room, and (v) the radiochemistry laboratory. All parts will be connected by Internet (TCP/IP), MIL-bus or serial interfaces. We plan to have two main control PCs, one for the gas-vacuum system and the second one to control magnets and for beam monitoring. The latter one will work as a server. All other computers, linked by TCP/IP protocol, will have the possibility to read data from these main

computers to visualize the actual status of the TASCA operation.

The Magnet control system consists of a low-speed control shell (0.1-0.5Hz control and visualization frequency) operated under LabVIEW installed in a PC. Connections to the magnet power supplies are made by PC cards via MIL-bus. The main program will work as a server and it will solely control the power supplies. These two connected to the quadrupoles allow maximum currents of 630 A while the third one for the dipole is limited to 700 A. All power supplies are located in the cellar. Tests of the quadrupole power supplies show good short and long term stabilities ( $< 10^{-5}$ ).

A 3-channel Tesla-meter will be used for magnetic field measurements. Connected to the control system by a serial port or ADC PC-card, it will be part of the online experimental monitoring.

The gas-vacuum control subsystem, including its differential pumping aspects, will be described in [2].

Beam current readings from collimators, Faraday cups and the beam dump are based on readouts from charge-frequency converters (QFCs). In addition, a beam current transformer will allow continuously monitoring the beam. Wire grids and luminescent screens are installed to properly focus the beam. This information will be visualized in the control room.

## References

- [1] M. Schädel et al., contribution to this report.
- [2] A.Semchenkov et al., contribution to this report

## Modelling the Differential Pumping of the TASCA Gas-Vacuum System

A. Semchenkov<sup>1,2</sup>, W. Bröchle<sup>1</sup>, E. Jäger<sup>1</sup>, E. Schimpf<sup>1</sup>, M. Schädel<sup>1</sup>, A. Türler<sup>2</sup>, A. Yakushev<sup>2</sup>  
<sup>1</sup>GSI, Darmstadt, Germany, <sup>2</sup>TUM Garching, Germany

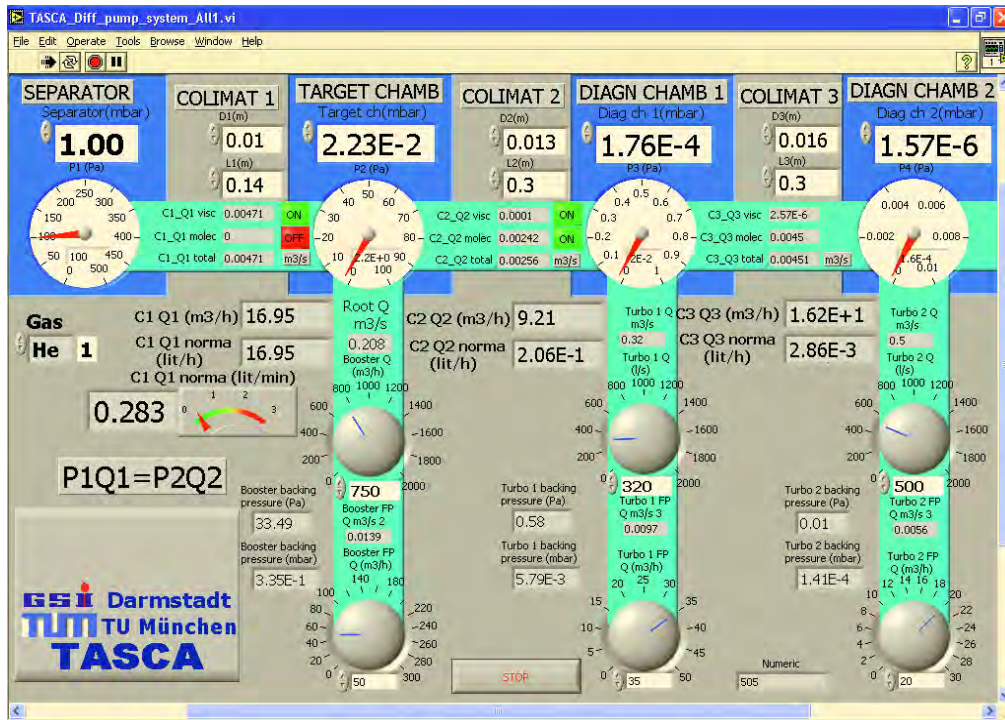


Fig. 1. User interface of the program to model the differential pumping situation at TASCA

The scientific program at the TASCA gas-filled separator [1] requires the highest possible UNILAC beam intensities. Presently, they are of the order of one particle microampere and a significant increase is in preparation. To make use of these intensities a windowless differential pumping system (DPS) was installed and a computer program was developed to simulate vacuum conditions at various sections along the beam line as a function of parameters like gas composition and pressure in the separator, pumping capacity and the geometry of the collimator; see Fig. 1 for the program interface. The goal was to maintain a stable pressure in the separator (typically about 1 mbar He) and get a rapid pressure drop over a short distance to obtain  $10^{-6}$  mbar in the beam line.

The system consists of three pumping sections and our design strongly profited from the experience obtained at RITU [2]. Our first section will have a 1070 m<sup>3</sup>/h (volume flow rate, N<sub>2</sub>) Roots pump with a 62 m<sup>3</sup>/h backing pump (test and comparisons with simulations were performed with smaller pumps). The second section has a 400 L/s (N<sub>2</sub>) turbomolecular pump with the specific feature that it can operate at a relatively high pressure coupled to a 32 m<sup>3</sup>/h backing pump. The third section consists of a 1400 L/s (N<sub>2</sub>) turbo and a 20 m<sup>3</sup>/h backing pump.

One envisioned configuration, which is depicted in Fig. 1, has collimators of 10x140, 13x300 and 16x300 (inner diameter x length / mm). Calculations with the DPS simu-

lation program show a pressure drop of about a factor 100 for each section; see Fig. 1. The program is written in LabVIEW and was tested experimentally with different gases. A good agreement between calculated and measured pressures was obtained. The program calculates the pressure and flow through collimators in a static regime of selected gases based on the following equations:

1. For viscous flow:

$$Q_v = (\pi D^4 \Delta P) / (256 \eta L),$$

with  $\eta$ : viscosity of gas at  $t=20^\circ\text{C}$ ,  $D$ : collimator diameter [m],  $L$ : collimator length [m],  $P$ : pressure [Pa].

2. For molecular flow:

$$Q_m = (1/6)(2\pi K T / M)^{1/2} (D^3 / L),$$

with  $K$ : Boltzmann constant,  $T$ : absolute temperature [K],  $M$ : mass of one molecule of gas [kg].

Set parameters of the program are the pressure in the separator, the filling gas, the collimator size and the pumping speed.

### References

- [1] M. Schädel et al., contribution to this report.
- [2] J. Uusitalo, [http://www-wnt.gsi.de/tasca04/images/contributions/4.1\\_Uusitalo.pdf](http://www-wnt.gsi.de/tasca04/images/contributions/4.1_Uusitalo.pdf)

## TASCA Target Group Status Report

K. Eberhardt, J. V. Kratz, D. Liebe, P. Thörle, Johannes Gutenberg-Universität, Mainz (UMZ)  
 H.-J. Maier, J. Szerypo, Sektion Physik, Ludwigs-Maximilians-Universität München, (LMU)  
 W. Brüchle, Ch. Düllmann, W. Hartmann, A. Hübner, E. Jäger, B. Kindler, B. Lommel,  
 M. Schädel, B. Schausten, E. Schimpf, A. Semchenkov, J. Steiner, GSI, Darmstadt, Germany  
 A. Türler, A. Yakushev, Institut für Radiochemie, Technische Universität München (TUM)  
 K. E. Gregorich, R. Sudowe, Lawrence Berkeley National Laboratory, Berkeley (LBNL)

The Trans-Actinide Separator and Chemistry Apparatus **TASCA** is currently installed at cave X8 and is dedicated to investigate the chemical and physical properties of the heaviest elements. An overview of the current status is given in a separate report [1].

For the production of Rf and Db isotopes, cold fusion reactions can be applied using Ti-beams with Pb- or Bi targets, respectively. Low melting metals can be substituted by compounds for application in high intensity beams [2]. However, to produce longer-lived isotopes of neutron-rich heavier actinides and transactinides hot fusion reactions with actinide targets are required. Here, possible target materials range from Th up to Cm or heavier elements.

We combined the different methods and capabilities of the four target laboratories involved to solve the challenging task of developing appropriate backings and targets. For first tests, we kept the geometry of the existing target wheel of the nuclear chemistry experiments at GSI unchanged. As we plan to install thinner backings for TASCA – so far 15 to 20  $\mu\text{m}$  thick Be foils were used - it is necessary to fix the backing on an adequate frame, as can be seen in Figure 1.

Al backings and Ti backings, supplied from different companies with different qualities, were produced by cold rolling. C backings were produced by resistance heating and applied without annealing. After two test beam times with  $^{12}\text{C}$  beam (500 pA) and  $^{40}\text{Ar}$  beam (800 pA), we now focus on 3  $\mu\text{m}$  Ti or 35  $\mu\text{g}/\text{cm}^2$  annealed C, alternatively, which will be tested with thermally evaporated  $\text{UF}_4$ , a target material in the near future.

As the target laboratory at GSI is specialised in evaporation, sputtering, and rolling of stable elements up to natural uranium, the foils discussed above were prepared there. The other three laboratories have the expertise of handling highly radioactive materials including the chemical purification of target material and the recovery of rare target material from used targets. After the decision for the appropriate backing has been made, backing foils will be given to the target laboratory at the LMU, where radioactive targets (Ra, Ac, Th, U, Pu, Cm) can be prepared by microevaporation. The group at the TUM offers the analytical capabilities to measure concentra-

tions of actinide elements in solution (also Pu, Cm). For the nuclear chemistry experiments at GSI the radioactive actinide targets are prepared by electrochemical deposition at UMZ.

The search for optimal conditions for the electrochemical deposition of U (as uranyl nitrate) from organic solution by molecular plating on thin Al- and Ti-backing foils is currently going on at LBNL and UMZ [3]. Figure 1 shows a picture of a 265  $\mu\text{g}/\text{cm}^2$   $^{238}\text{U}$ -layer produced by molecular plating on a 25  $\mu\text{m}$  thick Al-backing [3]. Target performance - when exposed to an ion beam - has not been tested yet. At UMZ a new electrochemical cell for improved deposition yield and uniformity of the target layer is under construction based on the design and the experience obtained at RIKEN [4]. Furthermore, optical microscopy, electron microscopy, and energy dispersive x-ray analysis are used for monitoring target thickness, chemical purity and homogeneity of the target surface. UMZ is testing a commercially available autoradiographic imager (Packard Instant Imager).

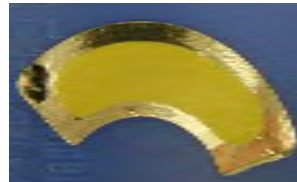


Figure 1:  $^{238}\text{U}$ -target (265  $\mu\text{g}/\text{cm}^2$ ) produced by molecular plating of uranyl nitrate from isobutanoic solution.

A new target station for TASCA is currently developed at GSI. This device is designed so that it can be used with the existing rotating actinide target wheel from GSI and with the new rotating target wheel system that is presently under development at LBNL for the Berkeley Gas-filled Separator (BGS), as well.

All contributions to the TASCA Working Group meetings and Workshops are accessible via [www-w2k.gsi.de/tasca](http://www-w2k.gsi.de/tasca).

### References

- [1] M. Schädel et al., this report
- [2] B. Kindler et al., accepted for NIM A
- [3] D. Liebe et al., this report
- [4] H. Haba, TASCA 05, Oslo, 2005;  
[http://www-w2k.gsi.de/tasca05/images/contributions/TASCA05\\_Haba.pdf](http://www-w2k.gsi.de/tasca05/images/contributions/TASCA05_Haba.pdf)

# Fully Relativistic *ab initio* Calculations of the Electronic Structures of the Superheavy Atoms

V. Pershina, GSI, Darmstadt, Germany  
E. Eliav, U. Kaldor, Tel Aviv University, Israel

In order to obtain accurate results from quantum chemical calculations on systems containing heavy atoms, relativistic effects must be accounted for in a most straightforward way. This can be achieved via the four-component formulation applying original Dirac formalism with almost no approximations. Due to a considerable software development effort in recent years, two of those quantum chemical codes exist, one of them being a product of a European collaboration, called the DIRAC package [1]. In the present work we have performed calculations of ionization potentials (IP) and electron affinities (EA) of the heaviest atoms Rf through Ds using the DIRAC program. The EAs of all the elements and correlated IPs of Mt and Ds were calculated for the first time.

In the basis of the method lies the many-electron relativistic Dirac-Coulomb (DC) Hamiltonian

$$H_{DC} = \sum_i h_D + \sum_{i<j} 1/r_{ij}, \quad (1)$$

where

$$h_D = c\vec{\alpha} \cdot \vec{p} + \beta c^2 + V_{nuc}. \quad (2)$$

The four-component orbitals are spinors

$$\phi_{nk} = \begin{pmatrix} P_{nk}(r) \\ Q_{nk}(r) \end{pmatrix}, \quad (3)$$

where  $P_{nk}(r)$  and  $Q_{nk}(r)$  are large and small component, respectively. The uncontracted Gaussian-type 33s29p20d16f9g universal basis set from [2] has been used for Rf through Ds. Though DIRAC has options to treat electron correlation at various levels of accuracy, MP2, CI (configuration interaction) and CC (coupled cluster), the calculations were performed for a small CI (treating open 7s, 6d and 7p shells as an active space) due to the limited capacity of a GSI 64-bit computer kindly offered to us by the theory department.\* In addition, multireference CC, the most accurate scheme, is presently applicable only to elements with two or less valence electrons or holes beyond a closed shell, e.g., for elements 104, 111 and 112. Work on overcoming this limitation is presently in progress in TAU, Israel. The DC CI calculated IPs and EAs are given in Table 1 and Fig. 1 in comparison with IPs calculated using numerical multiconfiguration Dirac-Fock (MCDF) [3] and DCB Fock-space CC [4] methods for some elements.

\*The author is thankful to the theory department (Prof. J. Knoll) and computing center for support. Calculations were also partially performed at computers of TAU, Israel.

Elements	IP			EA
	DC CI	MCDF [3]	CCSD [4]	DC CI
Rf	5.23	5.54	6.01	-0.10
Db	5.84	6.10	-	-0.15
Sg	6.49	7.03	-	-0.41
Bh	6.34	6.82	-	+0.17
Hs	6.35	6.69	-	-0.20
Mt	6.56	-	-	-0.23
Ds	6.68	-	-	-0.27

Our DC CI results for Rf through Hs are almost as accurate as MCDF obtained with a very large number of configurations and the trends in the row nicely agree.

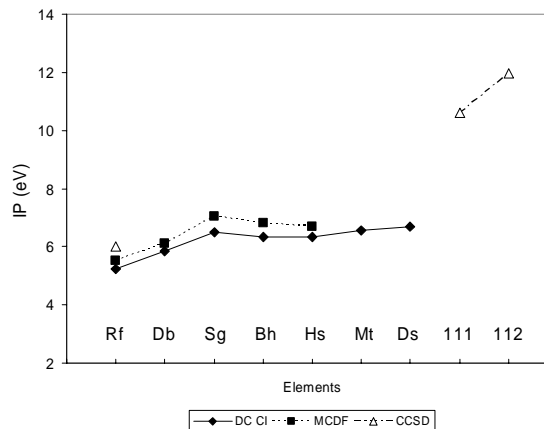


Figure 1: DC CI ionization potentials for elements Rf through 112 as compared to MCDF [3] and CCSD [4].

Thus, the results are very encouraging and we plan to perform large-scale CI calculations which will give even more accurate IPs and EAs (some might become positive), which will allow us to accurately determine some other important chemical properties of the heaviest elements like, e.g., chemical potentials. Further on, *ab initio* calculations for molecules of the heaviest elements using the DIRAC package are foreseen provided a 64-bit computer with the proper memory is at our disposal.

## References

- [1] DIRAC 04, written by H.J. Ja. Jensen, *et al.* (2004).
- [2] G.L. Malli, *et al.*, Phys. Rev. A **47** (1993).
- [3] E. Johnson, *et al.* J. Chem. Phys. **93**, 8041 (1990); B. Fricke, *et al.* Radiochim. Acta, **62**, 17 (1993); E. Johnson *et al.* J. Phys. Chem. A **42**, 8458 (1999).
- [4] U. Kaldor and E. Eliav, Adv. Quant. Chem. **31**, 313 (1998).

## Adsorption of Element 112 on a Au (100) surface

C. Sarpe-Tudoran<sup>1</sup>, V. Pershina<sup>2</sup>, B. Fricke<sup>1</sup>, J. Anton<sup>1</sup>

<sup>1</sup>Universität Kassel, D-34109 Kassel, <sup>2</sup>Gesellschaft für Schwerionenforschung, D-64291 Darmstadt

Element 112 is located in the Periodic system at the end of the 6d-series having a closed 6d and 7s shell [1]. This structure probably leads to a chemical behaviour which is expected to be somewhere between that of its homologue Hg and that of the noble gas Rn [2]. A summary of the state of the art of superheavy elements is given in Ref. [3].

In order to learn about the chemistry of this element already a number of years ago the experimental chemical groups which collaborate to detect the chemical behaviour of the superheavy elements have proposed to measure the position of the adsorption of element 112 in a thermochromatographic column.

In order to give a quantitative prediction for the adsorption energy of this element 112 on a gold (100) surface we have tried to finish our calculations and to present a final value. Due to the fact that there is no full relativistic solid state program available which is able to calculate this value we expanded our relativistic molecular density-functional code to tackle this problem [4].

Two methods are possible: The first is the calculation of larger and larger cluster which simulate the surface and then perform a calculation where the adatom is included on the surface. The difference of these total energies is by definition the adsorption energy. In order to accelerate the convergence with the cluster size, the above method is modified by adding many atoms around the inner cluster, which contribute only with their static potentials. This second method is the so called embedded cluster method.

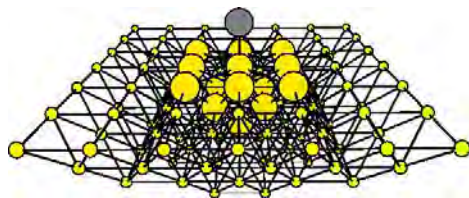


Figure 1: Structure of the atoms in the embedded cluster calculation for the case  $\text{Au}_{14}(9, 4, 1)$ .

A first prediction of the method 1 using the results for smaller clusters has been presented in a recent publication [5].

The main problem with both methods is the fact that the final result still was dependent on the cluster size and no convergence with the number of atoms in the cluster had been reached. The achievement of the last year is the fact that the difference of the adsorption energies of the two considered adsorbates became constant relative to the cluster size.

The results of our calculations are shown in Table 1 for the three possible adsorption sites on a Au (100) surface:

Table 1: Adsorption energy of Hg and Element 112 on a (100) gold surface, for different adsorption sites.

top		bridge		hollow	
System	En. [eV]	System	En. [eV]	System	En. [eV]
$\text{Au}_{14}\text{Hg}$	1.64	$\text{Au}_{14}\text{Hg}$	1.68	$\text{Au}_{21}\text{Hg}$	0.86
$\text{Au}_{14}112$	1.47	$\text{Au}_{14}112$	1.18	$\text{Au}_{21}112$	0.82
$\text{Au}_{34}\text{Hg}$	1.02	$\text{Au}_{20}\text{Hg}$	1.31	$\text{Au}_{29}\text{Hg}$	0.84
$\text{Au}_{34}112$	0.65	$\text{Au}_{20}112$	0.96	$\text{Au}_{29}112$	0.74
		$\text{Au}_{36}\text{Hg}$	1.52		
		$\text{Au}_{36}112$	1.16		

top, bridge and hollow. The absolute values of the adsorption energies in eV of the elements Hg and 112 calculated in the GGA approximation (with B88 functional for exchange and P86 for correlation) are given.

First consequence of these calculations can be drawn from the absolute values of the adsorption energies. According to these data the "bridge" adsorption site is the preferred one. That is the reason why we have expanded our calculations to the very large  $\text{Au}_{36}$  cluster. The difference between the binding energies of Hg and Element 112 is the same for the clusters with 20 and 36 atoms, namely  $\approx 0.35$  eV. This number together with the experimental adsorption energy of Hg on Au surface (0.92 eV, reference [6]) allows us to estimate the adsorption energy of Element 112 on such a surface, namely 0.58 eV.

### References

- [1] B. Fricke, *Structure and Bonding* **21**, 89 (1975)
- [2] R. Eichler, M. Schädel, *GSI Scientific Report*, (2001), p. 185
- [3] Schädel, Matthias (Ed.), *The Chemistry of Superheavy Elements* (Ed.), Kluwer Academic Publisher, (2003)
- [4] T. Jacob, J. Anton, C. Sarpe-Tudoran, et. al. *Surf. Sci.*, **536**, 45–54 (2003)
- [5] V. Pershina, T. Bastug, C. Sarpe-Tudoran et al., *Nucl. Phys. A*, **734**, 200 (2004)
- [6] J.-P. Niklaus, R. Eichler, S. Soverna, H. W. Gäggeler, *PSI Annual Report*, 8 (2000)

## Theoretical Predictions of Complex Formation of Group-4 Elements Zr, Hf, and Rf in H<sub>2</sub>SO<sub>4</sub> Solutions

V. Pershina, GSI, Darmstadt, Germany

D. Polakova, J. P. Omtvedt, Oslo University, Norway

Complex formation of Zr, Hf, and Rf in HF and HCl solutions has been studied both experimentally and theoretically [1,2]. Trends in  $K_d$  (distribution coefficient) values evidencing the strengths of formed complexes were shown to be influenced by such factors as pH of solution and acid concentration. Presently, experiments are under way to investigate complex formation of these elements in H<sub>2</sub>SO<sub>4</sub> solutions using the SISAK technique [3]. To predict the outcome of these experiments, the present theoretical study has been undertaken. Accordingly, calculations of the free energy change,  $\Delta G^f$ , of the following complex formation reactions were performed:



Electronic structures of the following complexes formed at various H<sub>2</sub>SO<sub>4</sub> concentrations were calculated using the fully relativistic (4-component) density functional theory method (4c-DFT) [4]: M(SO<sub>4</sub>)(H<sub>2</sub>O)<sub>6</sub><sup>2+</sup>, M(SO<sub>4</sub>)<sub>2</sub>(H<sub>2</sub>O)<sub>4</sub>, M(SO<sub>4</sub>)<sub>3</sub>(H<sub>2</sub>O)<sub>2</sub><sup>2-</sup>, where M = Zr, Hf, and Rf. Electronic structures of hydrated and hydrolyzed complexes of these elements were calculated earlier [5].

$\Delta G^f$ s were calculated via the model described in [5] as a sum of the ionic,  $\Delta E^C$ , and covalent,  $\Delta E^{OP}$ , constituents. Both  $\Delta E^C$  and  $\Delta E^{OP}$  were determined via Mulliken analysis implemented in the DFT method. Geometrical configurations of the complexes were chosen on the basis of an analysis of solid-state structure data of Zr sulphuric complexes. Bond lengths in the Hf and Rf complexes were estimated using optimized bond lengths in simpler gas-phase compounds and in accordance with ionic radii. The calculated  $\Delta G^f$  for reactions of types (1) and (2) are summarized in Tables 1 and 2.

Table 1. Coulomb parts of the free energy change,  $\Delta E^C$  (in eV), for reactions of type (1)

Complex	Zr	Hf	Rf
M(SO <sub>4</sub> )(H <sub>2</sub> O) <sub>6</sub> <sup>2+</sup>	-35.72	-35.84	-33.60
M(SO <sub>4</sub> ) <sub>2</sub> (H <sub>2</sub> O) <sub>4</sub>	-42.43	-42.43	-39.37
M(SO <sub>4</sub> ) <sub>3</sub> (H <sub>2</sub> O) <sub>2</sub> <sup>2-</sup>	-45.14	-45.02	-41.38

Thus, trends in the formation of the three types of complexes via reactions of type (1) are Hf > Zr >> Rf, Zr = Hf >> Rf and Zr > Hf >> Rf, respectively. For reactions of type (2), trends are Hf > Zr >> Rf, Hf > Zr >> Rf, and Zr > Hf >> Rf for the three types of complexes, respectively. The same trends should be observed for the  $K_d$  values,

since  $K_d \cong f(\beta_i)$ , and  $\log \beta_i = -\Delta G^f/2.3RT$ . The predicted  $K_d$  for Hf and Rf with respect to the measured  $K_d$  for Zr [6] in anion-exchange separations are shown in Fig. 1.

Table 2. Coulomb parts of the free energy change,  $\Delta E^C$  (in eV), for reactions of type (2)

Complex	Zr	Hf	Rf
M(SO <sub>4</sub> )(H <sub>2</sub> O) <sub>6</sub> <sup>2+</sup>	-31.03	-31.23	-29.49
M(SO <sub>4</sub> ) <sub>2</sub> (H <sub>2</sub> O) <sub>4</sub>	-37.74	-37.82	-35.26
M(SO <sub>4</sub> ) <sub>3</sub> (H <sub>2</sub> O) <sub>2</sub> <sup>2-</sup>	-40.45	-40.41	-37.27

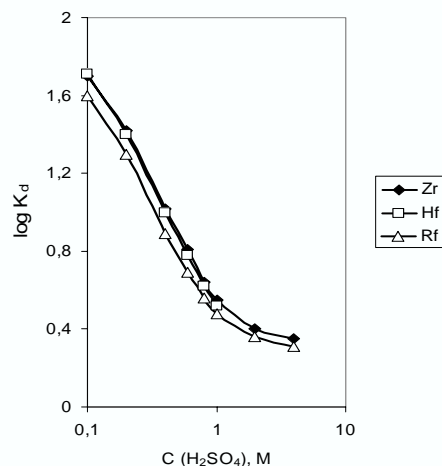


Figure 1: Predicted  $K_d$  values for Hf and Rf with respect to  $K_d$ s of Zr [6] in anion-exchange separations

Thus, trends in  $K_d$  of Zr and Hf are dependent on the pH of solution. With increasing H<sub>2</sub>SO<sub>4</sub> concentration it should be Zr > Hf in agreement with experiments [6]. Complexes of Rf should be weaker than those of Zr and Hf at all pH, so that  $K_d(\text{Zr}) > K_d(\text{Hf}) \gg K_d(\text{Rf})$  at the whole range of acid concentrations. The recent SISAK experiment on Rf confirmed this trend.

### References

- [1] J.V. Kratz in: "The Chemistry of Superheavy Elements", ed. M. Schädel, Kluwer, (2003), p. 159.
- [2] V. Pershina, *ibid*, p. 31.
- [3] J. P. Omtvedt, *et al.* J. Nucl. Radiochem. Sci. **3**, No. 1, (2002).
- [4] T. Bastug, *et al.* Phys. B **28**, 2325 (1995).
- [5] V. Pershina *et al.* Radiochim. Acta **90**, 869 (2002).
- [6] R. Caletka, *et al.* J. Rad. Nucl. Chem. **142**,383 (1990).